Check for updates

Received: 10 August 2023 | Revised: 17 October 2023 | Accepted: 18 October 2023

DOI: 10.1002/cjce.25136

RESEARCH ARTICLE

THE CANADIAN JOURNAL OF CHEMICAL ENGINEERING

tert-butanol and hydrogen peroxide react over Amberlyst-15 to form *tert*-butyl hydroperoxide

Marie-Thérèse El Kfoury | Olga V. Chub | Daria C. Boffito | Gregory S. Patience

Chemical Engineering, Polytechnique Montréal, C.P. 6079, Succ. "CV", Montréal, Quebec, Canada

Correspondence
Gregory S. Patience, Chemical Engineering, Polytechnique Montréal, C.P. 6079, Succ. "CV", Montréal, H3C 3A7 QC, Canada.
Email: gregory-s.patience@polymtl.ca

Funding information
Arkema, Grant/Award Number: DB/CDT 04 5959; Mitacs, Grant/Award Number: IT18514

Abstract

Organic peroxides are explosive compounds that are applied as disinfectants, bleaching agents, and as initiators for polymer synthesis because of their high reactivity. Traditional homogeneous processes with H_2SO_4 catalyst produce salts, either in the neturalization step after reaction or due to the foramtion of *tert*-butyl hydrogen sulphate, that must be disposed of, which introduces cost and represents an environmental burden. Here, we devised a flow chemistry approach to oxidize *tert*-butyl alcohol (TBA) to *tert*-butyl hydroperoxide (TBHP) over various heterogeneous catalysts. Under acidic conditions, TBHP is the main product and di-*tert*-butyl peroxide (DTBP) and peroxy-ketal are by-products. The most active catalyst was Amberlyst-15, while yield of Nafion, activated carbon, and heteropoly acids (HPA) on carbon and silica matrices was less than 1% at 70°C. In in the range of 30 to 50°C, a first order kinetic expression characterizes the *tert*-butyl alcohol conversion well ($R^2 = 0.99$). The reaction rate is slow and the rate constant, $k_{40°C}$, was 0.003 min^{-1}. Above 50°C, by-products reacted further to acetone, methane, ethane, and other compounds.

KEYWORDS

heterogeneous catalysis, hydrogen peroxide, kinetics, *tert*-butyl alcohol, *tert*-butyl hydroperoxide

1 | INTRODUCTION

Because of their reactivity, organic peroxides are efficient disinfectants and bleaching agents. At the commercial scale, the polymer industry is the main consumer of organic peroxides as initiators.[1] The market is expected to increase by 3.7% per annum until 2027 and much of the growth is attributable to these applications.[2] H_2O_2 partially oxidizes organic compounds to produce peroxides—hydroperoxides, diperoxides, peracids, peroxy esters, and peroxy ketals.

Traditional approaches rely on homogeneous systems to add H_2O_2 to electron rich molecules like alkenes, alcohols, and ethers.[3,4] Texaco Chemicals introduced a process to produce *tert*-butyl hydroperoxide (TBHP) from oxygen and isobutane without any catalyst, but with di-*tert*-butyl peroxide (DTBP) as initiator.[5] TBHP yield reached 10% after 5 h. Distillation columns or solvent extractors separate the main product from the mixture. Vapour phase conversion of isobutane reached 25% with molecular oxygen and hydrogen bromide as a catalyst.[6] With excess H_2O_2, Shell achieved 95% TBHP yield

This is an open access article under the terms of the Creative Commons Attribution License, which permits use, distribution and reproduction in any medium, provided the original work is properly cited.
© 2023 The Authors. *The Canadian Journal of Chemical Engineering* published by Wiley Periodicals LLC on behalf of Canadian Society for Chemical Engineering.

with Friedel-Crafts halides and inorganic acid catalysts.[7] Research Corporation produced the mono-alkyl salt, from an alcohol or an unsaturated hydrocarbon with sulphuric acid.[8] The salt then reacts with H_2O_2 at 0°C to form alkyl hydroperoxide. Via a one-step reaction, Frenkel and Pettijohn[9] isolated the hydroperoxide or diperoxide from the mixture containing *n*-alkyl or *t*-alkyl ether, an RO_2H compound and an acid catalyst. Depending on R, whether it is hydrogen or *tert*-alky, they obtained *tert*-alkyl hydroperoxide or di-*tert*-alkyl peroxide.

The drawback of homogeneous catalysis includes the difficult separation of the catalyst from the mixture, its neutralization, disposal, and safety issues. Liquid heterogeneous catalytic processes circumvent some of these limitations. Heterogeneous superacids include polymer resins sulfonic acids, graphite intercalated acids, and heteropoly acids (HPA).

Ion exchange resins are gaining interest as catalysts for organic synthesis. The chlorination, fluorination, and nitration of benzene rings improve the stability and acidity of these sulfonated resins.[10] Active sulfonic acids mounted on the macroreticular styrene divinylbenzene matrix makes the acidity of Amberlyst-15 catalyst comparable to sulphuric acid.[11] It is efficient for esterification, transesterification, Friedel-Crafts alkylation, acylation, halogenation, and nucleophilic substitution reactions.[12]

The poly-tetrafluoroethylene backbone with perfluorovinyl ether sulfonate end groups make Nafion a very strong acid with a $pK_a \approx -6$.[13] It was first developed by DuPont in the 1970s. Its low price, high proton conductivity, and good chemical and mechanical stability make it efficient in fuel cells, energy storage devices, and dryer membranes.[14,15] On the contrary, its high swelling capacity and water sorption limit its applications in certain areas.[16]

Motivated by environmental constraints, industry continues to develop alternatives—heterogeneous catalysis, heteropolyacids—to replace homogeneous processes. Heteropolyacids are recyclable, insoluble in apolar solvents, and highly stable with respect to air and humidity. HPA showed higher selectivity and yields with low reaction times than conventional H_2SO_4, HCl and Lewis acid catalysts.[17] Four types of HPA exist where the Keggin type (formula $H_xA_yPW_{12}O_{40}$) is frequently applied in oxidation reactions.[18]

Finally, activated carbon is a good heterogeneous catalyst and catalytic support for various reactions. Due to its stability in both acidic and basic media, it is applied for oxidation, reduction, acid catalyzed, basic catalyzed reactions, and C—C bond formation reactions as polymerization of cycloalkenes and dehydrogenation of alcohols.[19]

Although their industrial interest is high, peroxides are unstable and violently decompose when exposed to heat, friction, and shock. Aqueous TBHP is more hazardous than TBHP solutions with acids/alkali; it thermally explodes with a sharp self-heating rate ($T_{max} = 336^\circ C$) under adiabatic conditions.[20,21] At 49.5°C, TBHP with *p*-toluene sulphonic acid decomposes to DTBP and H_2O_2 or to methanol and acetone via a radical mechanism. Acetone reduces the stability of the mixture and decreases the decomposition temperature to 31°C.[22] The unimolecular scission of the peroxy bond of TBHP is first order according to Willms et al.'s DSC study.[23] DTBP decomposes via the O—O weak bond fission to two *tert*-butoxy radicals with the lowest barrier of 44 k cal mol^{-1}.[24]

Industry is motivated to reduce its environmental footprint to produce organic peroxides and replace liquid phase homogeneous processes that produce salt with a heterogeneous route. Here we synthesized TBHP from *tert*-butyl alcohol (TBA) and H_2O_2 via a heterogeneous pathway in a fixed-bed reactor. The focus has been to screen many catalyst compositions (six in total) to identify likely candidates for further development and optimization. For this reason, the experimental protocol included just three operating temperatures, two flow rates, and two TBA concentrations. Since the work was directed at screening catalyst, the experimental plan was restricted to low conversion. Of the six catalysts, only Amberlyst-15 had any appreciable selectivity to TBHP ($<50\%$). We estimated the apparent kinetic parameters of the reaction and proposed a mechanism that accounted for the trends.

2 | EXPERIMENTAL

2.1 | Chemicals

tert-butyl alcohol (ACS reagent, ≥99.7%), hydrogen peroxide (50% in H_2O), ethanol (ACS spectrophotometric grade, 95%), 2-propanol (≥99.5%), Amberlyst-15 hydrogen form, and Nafion NR50 (pellets) were purchased from Sigma Aldrich. We used them without further purification. For the home-made catalysts, the precursors include tungstophosphoric acid (reagent grade), caesium carbonate (99%), silica gel, and activated carbon also from Sigma Aldrich.

2.2 | Laboratory set up

Before initiating the reaction, we diluted the H_2O_2 solution to 30% in distilled water. Then we mixed melted TBA (at 50°C) with the hydrogen peroxide solution in an

1939019x, 0, Downloaded from https://onlinelibrary.wiley.com/doi/10.1002/cjce.25136 by Ecole Polytechnique De Montreal, Wiley Online Library on [24/11/2023]. See the Terms and Conditions (https://onlinelibrary.wiley.com/terms-and-conditions) on Wiley Online Library for rules of use; OA articles are governed by the applicable Creative Commons License

equimolar ratio. A J-Kem dual syringe pump fed the reagents to the bottom of the fixed-bed reactor made of stainless steel compatible with peroxides. Coating vessels with polyethylene, polytetrafluoroethylene (PTFE), or polyether ether ketone (PEEK) reduces the catalytic decomposition of TBHP. However, coating is more critical in the isobutane oxidation process that operates at 140°C.[25] Selectivity in a Ti reactor reached 56% at 25% conversion versus only 43% in a stainless steel vessel.[26] We loaded it with 0.3 g of catalyst. Iso-propanol trapped and cooled the reaction products down to 0°C to prevent any decomposition (Figure 1).

To identify optimal reaction conditions, we first conducted experiments at 40, 55, and 70°C. We tested 1 and 2 mL min^{-1} flow rates at the two best temperatures. Finally, we examined Amberlyest-15, Nafion, $Cs_{2.5}H_{0.5}PW_{12}O_{40}/SiO_2$, $Cs_{2.5}H_{0.5}PW_{12}O_{40}/C$, $Cs_{2.5}H_{0.5}PW_{12}O_{40}$/Amberlyst-15, and activated carbon at the optimal temperature and flow rate.

2.3 | Catalyst synthesis and characterization

We synthesized three home-made catalysts besides the commercially available samples: caesium salt of tungstophosphoric acid ($Cs_{2.5}H_{0.5}PW_{12}O_{40}$) impregnated on either silica, activated carbon, or Amberlyst-15.

The incipient wetness impregnation technique is applied for supported HPA. In the first step of the $Cs_{2.5}H_{0.5}PW_{12}O_{40}/SiO_2$ synthesis, we impregnated the tungstophosphoric acid on silica powder, dried it at 110°C for 4 h, and calcined it at 300°C for 6 h. In the same way, we impregnated the caesium carbonate on the HPA/SiO_2, dried it at 110°C, and calcined it at 300°C.[27]

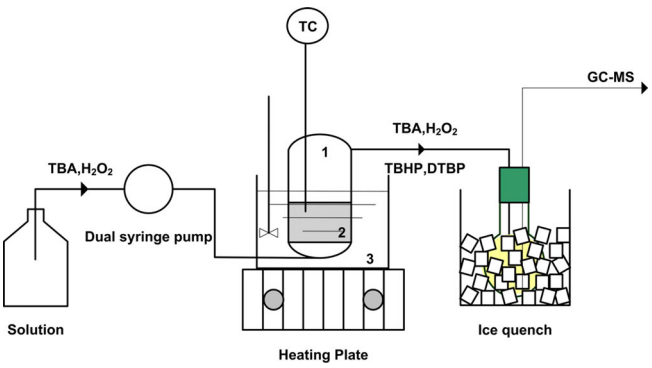

FIGURE 1 Scheme of lab-scale process; 1: fixed-bed reactor filled with 2: Amberlyst-15 is immersed in 3: magnetically stirred, heated water bath. DTBP, di-*tert*-butyl peroxide; GC–MS, gas chromatography–mass spectrometry; TBA, *tert*-butyl alcohol; TBHP, *tert*-butyl hydroperoxide; TC, temperature control.

For the $Cs_{2.5}H_{0.5}PW_{12}O_{40}/C$ catalyst, we followed the method reported by Yang et al.[28] First, we impregnated the $Cs_{2.5}H_{0.5}PW_{12}O_{40}$ salt for 6 h. Then, the black solid was washed in distilled water and dried at 105°C for 24 h. We applied the same impregnation method for the ($Cs_{2.5}H_{0.5}PW_{12}O_{40}$)/Amb-15 catalyst without prior treatment of Amberlyst-15.[29]

To determine the concentration of Brønsted acid sites in porous catalyst, we titrated 0.05 g Amberlyst-15 suspended and stirred in 5 mL of distilled water and 0.5 mL of NaOH (0.1 M) with HCl (0.1 M) in presence of phenolphthalein as indicator.[30] We stopped the titration when the solution changed from red rose to colourless.

2.4 | Characterization

Gas chromatography is widely applied for peroxide analysis for thermally stable compounds. So, low injection temperature and slow heating rates are suitable parameters for hydroperoxides.[31,32] We used both gas chromatography–mass spectrometry (GC–MS) and GC-flame ionization detection (FID) to quantify the liquid products at different stages.

A gas chromatograph Agilent (GC 7890A) with ultra-inert DB Wax column connected to a mass spectrometer 5975C VL MSD (Agilent) identified the liquid products of the reaction (Tables 1 and 2).

Helium passed through the column at 0.7 mL min^{-1}. The auto-sampler injected 0.2 μL in split mode (split ratio 50:1) where the sample heated to 77°C. The temperature in the oven ramped to 200°C over 27 min (Table 3).

In order to quantify the reaction products, we calibrated the GC–MS with standards and further diluted the

TABLE 1 Gas chromatography (GC) column's specs.

Parameter	Specification
GC tubing	Fused silica
Stationary phase	Polyethylene glycol
Interior diameter (mm)	0.25
Length (m)	30

TABLE 2 Mass spectrometry parameters.

Parameter	Value
Mass source temperature	230°C
Quad temperature	150°C
Trasfer line temperature	250°C
Full scheme range	29 to 500

1939019x, 0, Downloaded from https://onlinelibrary.wiley.com/doi/10.1002/cjce.25136 by Ecole Polytechnique De Montreal, Wiley Online Library on [24/11/2023]. See the Terms and Conditions (https://onlinelibrary.wiley.com/terms-and-conditions) on Wiley Online Library for rules of use; OA articles are governed by the applicable Creative Commons License

sample with ethanol. We calculated the concentrations of the products as in Equation 1:

$$C = F_{\text{calibration}} \cdot A_{\text{exp}} \cdot n_{\text{dilution}} \tag{1}$$

A slightly modified method applies also to the GC-FID CP-3800 equipped with the Agilent ultra-stable, ultra-inert DB-1MS column (15 m, 0.25 mm, 0.25 μm) but the auto-sampler injects 10 μL liquid products in 100:1 split mode and the helium passes at 1.3 mL min^{-1} here. Knowing that the boiling point of TBA and DTBP is 82 and 111°C,[33–35] respectively, the oven temperature ramps up to 200°C over 16 min to vaporize all the compounds (Table 4). The FID operates at a set-point of 250°C to minimize condensation.

2.5 | Apparent kinetic measurements

To derive the apparent kinetic parameters of the reaction, we designed a set of experiments in a batch reactor to operate in the range 30 to 70°C. For this, we mixed TBA and hydrogen peroxide in a 500 mL round flask containing 4 g of Amberlyst-15. In each run, the magnetic stirrer homogenized the solution at the set temperature. To derive the reaction rate, we sampled the products at 0, 15, 30, 45, and 60 min.

GC–MS is insensitive to H_2O_2, so we derived the kinetic model solely on the TBA signal. We carried out two sets of experiments with excess H_2O_2 at a molar ratio of H_2O_2 to TBA: 1.1 and 2 (varying the TBA concentration while maintaining the H_2O_2 constant). We derived the reaction rate constant k and activation energy E_a based on minimizing the sum of the square error applying a Levenberg–Marquardt algorithm[36]:

TABLE 3 Gas chromatography–mass spectrometry ramp conditions.

	Step 1	Step 2	Step 3
Rate (°C min^{-1})	N/A	5	20
T_{oven} (°C)	40	110	200
t_{hold} (min)	4	0	5

Abbreviation: N/A, not applicable.

TABLE 4 Gas chromatography–Flame ionization detection ramp conditions.

	Step 1	Step 2	Step 3
Rate (°C min^{-1})	N/A	20	20
T_{oven} (°C)	35	100	200
t_{hold} (min)	3	1	4

Abbreviation: N/A, not applicable.

$$k = k_0 \exp\left[-\frac{E_a}{R}\left(\frac{1}{T} - \frac{1}{T_0}\right)\right] \tag{2}$$

3 | RESULTS AND DISCUSSION

3.1 | Mechanism

Any surface reaction, in case of heterogeneous catalysts, occurs via one or a combination of the following three mechanisms. In the case of Langmuir–Hinshelwood mechanism, compounds A and B adsorb on the surface of the catalyst, collide, and form a new species A-B, which will subsequently desorb. Another case is based on the Eley–Rideal mechanism when only A adsorbs on the catalyst surface and B reacts with this surface adsorbed species to form A-B that then desorbs. Finally, the precursor mechanism occurs if A adsorbs to the surface and B collides with the surface to give a mobile precursor state that will facilitate the formation of the new A-B compound.[37]

In the case of this study, we presume the reaction rate between TBA and H_2O_2 is best modelled by the Eley–Rideal rate expression but two alternative mechanisms are possible. In the first (substitution), TBA adsorbs on the catalyst surface and reacts with the Brønsted acid site to form a *tert*-butyl ion. In this case, H_2O_2 in water dissociates via the O—H bond rather than the O—O bond with a low energy barrier of 35 kJ mol^{-1}.[38] Both hydroperoxyl and *tert*-butyl ions then collide and form the TBHP (Equations 3–5).

$$H_3C-\underset{\underset{CH_3}{|}}{\overset{\overset{CH_3}{|}}{C}}-OH \overset{H^+}{\rightleftharpoons} H_3C-\underset{\underset{CH_3}{|}}{\overset{\overset{CH_3}{|}}{C^+}} + HO^- \tag{3}$$

$$HOO-H \overset{H_2O}{\rightleftharpoons} HOO^- + H^+ \tag{4}$$

$$H_3C-\underset{\underset{CH_3}{|}}{\overset{\overset{CH_3}{|}}{C^+}} + HOO^- \rightarrow H_3C-\underset{\underset{CH_3}{|}}{\overset{\overset{CH_3}{|}}{C}}-OOH \tag{5}$$

An alternative (oxidation), perhaps more likely, is that H_2O_2 preferentially adsorbs on the sulphonic sites (Brønsted acid) of the Amberlyst-15 rather than TBA. The hemolysis of the H_2O_2 forms two $^{\cdot}OH$ species. $^{\cdot}OH$ then abstracts a H from TBA from the bulk liquid to form a *tert*-butyl radical.

For the other by-products, TBHP in the presence of H^+ dissociates via two mechanisms to give either DTBP

1939019x, 0, Downloaded from https://onlinelibrary.wiley.com/doi/10.1002/cjce.25136 by Ecole Polytechnique De Montreal, Wiley Online Library on [24/11/2023]. See the Terms and Conditions (https://onlinelibrary.wiley.com/terms-and-conditions) on Wiley Online Library for rules of use; OA articles are governed by the applicable Creative Commons License

or acetone. The decomposition to DTBP and H_2O_2 or to acetone and methanol occurs depending on the attack of H^+ to either the C—O bond or the O—O bond. Acetone increases the reactivity and the decomposition of TBHP in the presence of p-toluenesulphonic acid. In fact, H^+ reacts with the first oxygen of the hydroperoxide functional group and creates the H_2O_2 leaving group. This forms the *tert*-butyl ion which reacts again with TBHP to give DTBP[22]:

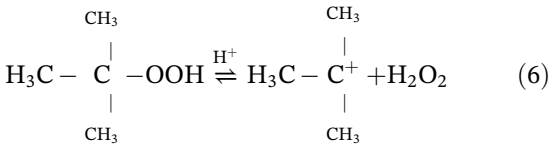

(6)

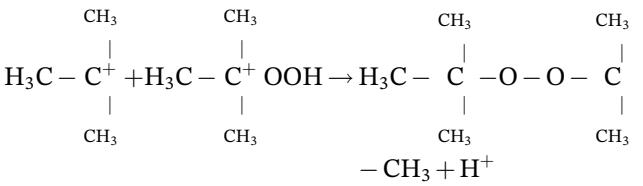

(7)

Also, H^+ can attack the second oxygen and creates a reactive intermediate inducing the 1,2 rearrangement to give acetone. However, acetone also reacts with two equivalents of TBHP to form the 2,2-bis(tertbutylperoxy) propane or the peroxyketal.[22]

3.2 | Chromatogram

The chromatogram (Figure 2) demonstrated the narrow symmetric peaks of DTBP (2.6 min), TBA (4.0 min), TBHP (15.5 min), and an undefined product eluted at 5.5 min from GC–MS. For the GC-FID chromatogram (Figure 3), the shift in retention time of all the compounds is due to two factors. The differences in the columns' stationary phases and lengths and the carrier gas flow rates shorten the retention time in the case of GC-FID. The DB-1MS column is 15 m shorter than the DB wax column. Also, the helium flow rate is 1.3 mL min^{-1}, higher than the one for GC–MS, meaning that the analytes are swept faster from the column and their retention time decreases. Coming back to the mechanism, we presume that the undefined product in GC–MS chromatogram is the peroxyketal as acetone elutes between 0 and 2 min in the case of DB Wax column, not at 5.5 min.

3.3 | Mass balance

Table 5 summarizes the conversion of TBA and the selectivity of both products TBHP and DTBP at various operating conditions. The expressions for the conversion and selectivity are as follows:

$$X_{\mathrm{TBA}} = \left(1 - \frac{n_{\mathrm{TBA\ out}}}{n_{\mathrm{TBA\ in}}}\right) \cdot 100 \tag{8}$$

$$S_{\mathrm{i}} = \frac{n_{\mathrm{i}}}{n_{\mathrm{TBA\ in}} - n_{\mathrm{TBA\ out}}} \cdot 100 \tag{9}$$

3.4 | Temperature and flow rate effect

Over the range of 40 to 70°C, the flow rate has a more pronounced influence on the extent of TBA conversion,

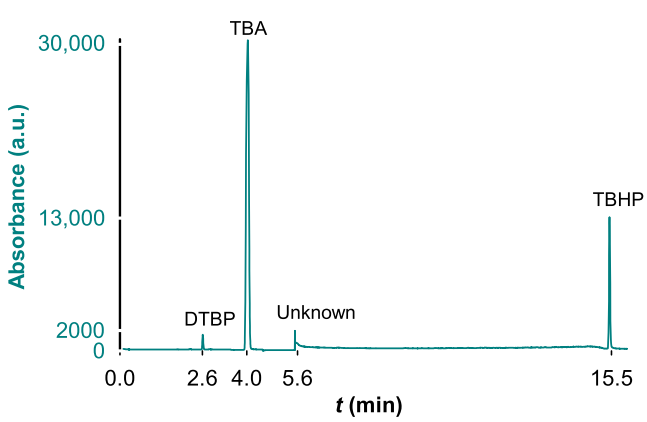

FIGURE 2 Gas chromatography–mass spectrometry chromatogram for the sample at 1 h and 50°C with a molar ratio of 2 (DB Wax column). DTBP, di-*tert*-butyl peroxide; TBA, *tert*-butyl alcohol; TBHP, *tert*-butyl hydroperoxide.

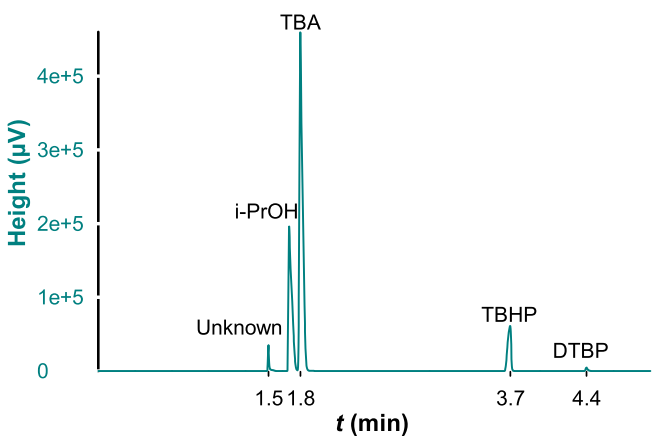

FIGURE 3 Gas chromatography-Flame ionization detection chromatogram for the sample at 1 h and 70°C at a flow rate of 1 mL min^{-1} (DB 1MS column). DTBP, di-*tert*-butyl peroxide; TBA, *tert*-butyl alcohol; TBHP, *tert*-butyl hydroperoxide.

1939019x, 0, Downloaded from https://onlinelibrary.wiley.com/doi/10.1002/cjce.25136 by Ecole Polytechnique De Montreal, Wiley Online Library on [24/11/2023]. See the Terms and Conditions (https://onlinelibrary.wiley.com/terms-and-conditions) on Wiley Online Library for rules of use; OA articles are governed by the applicable Creative Commons License

TABLE 5 Experimental results of the reaction of *tert*-butyl alcohol (TBA) (4.1 mol L^{-1}) with hydrogen peroxide (4.1 mol L^{-1} in H_2O) over various catalysts.

Catalyst	T (°C)	Q (mL min^{-1})	X_{TBA} (%)	S_{TBHP} (%)	Y_{TBHP} (%)	S_{DTBP} (%)
Amberlyst-15	40	1	9.6	4.6	0.4	0.2
Amberlyst-15	55	1	25.3	11.7	3	0.2
Amberlyst-15	70	1	52	30	16	6.4
Amberlyst-15	55	2	9.3	6.6	0.6	0.1
Amberlyst-15	70	2	24	22	5	0.4
Nafion	70	1	22	1.6	0.4	0.1
HPA/C	70	1	7.7	9.1	0.7	0.3
HPA/SiO_2	70	1	12	1.6	0.2	0.1
HPA/Amberlyst-15	70	1	11	44	5	0.7
Activated carbon	70	1	28	1.1	0.3	0.1

Abbreviations: HPA, heteropoly acids; DTBP, di-*tert*-butyl peroxide; TBA, *tert*-butyl alcohol; TBHP, *tert*-butyl hydroperoxide.

which suggests that the activation energy is low. The upper temperature was constrained by the stability of Amberlyst-15 below 120°C[39] and the decomposition temperature of TBHP that ranges from 77 to 110°C.[40] The yield of TBHP at 1 h increased from 0.5% to 3% and 16% when the temperature increases from 40 to 55 and 70°C, respectively. As expected for a first order reaction, the TBHP yield at a flow of 1 mL min^{-1} was higher than at 2 mL min^{-1}. We then selected 70°C and 1 mL min^{-1} as the optimum working conditions for TBHP synthesis (Figure 4).

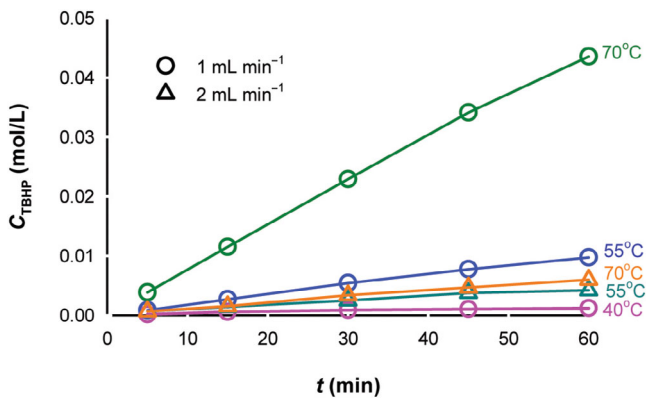

FIGURE 4 Formation of *tert*-butyl hydroperoxide (TBHP) as a function of time, temperature, and flow rate.

3.5 | Catalyst type effect

From the volumetric titration reported above, we obtained the equivalence at V_{eq} of 2.4 mL and calculated the Amberlyst-15 acidic concentration to 4.8 mmol g^{-1} as in Equation 10.

$$C_{\text{Brønsted acid}} = \frac{C_{HCl} \cdot V_{eq}}{m_{cat}} \tag{10}$$

The value agrees with data in the literature (4.3 mmolL^{-1}).[41,42] This high acidic concentration, in addition to the macroporous matrix and hydrophilic sites, explains the activity of Amberlyst-15. In fact, Amberlyst-15 is hydrophobic due to the styrene-based structure but the SO_3H functional group makes it hydrophilic and a leads to an affinity to polar molecules.[41] TBA, due to the polar hydroxyl group, may adsorb to the catalytic sites. However, Amberlyst-15 is also hygroscopic and adsorbs water.[43] This hinders the adsorption of TBA and deactivates the sulfonic groups, thereby limiting the conversion to 52% and the TBHP yield to 16% at 70°C (Figure 5).

Nafion was a disappointing catalyst for TBHP synthesis. The low TBA conversion over Nafion (22%) is due to the fact that alcohol preferentially adsorbs to the surface, which is a positive attribute. However, once adsorbed, TBA produces a $HO^{\cdot}$ radical that degrades Nafion. $HO^{\cdot}$ decomposes the support by removing a hydrogen from the carboxylic acid end group or from the hydrofluorocarbon. This will dissociate and shorten the backbone releasing HF molecules.[14]

The caesium salts of HPA are hydrophobic and adsorb water readily, which deactivates the catalyst.[17] In our case, the reagent solution has a H_2O mass fraction of 43%. Consequently, TBHP yield was only 0.2% (Figure 5).

Knowing that carbon entraps HPA in water, we tried it as a support for $Cs_{2.5}H_{0.5}PW_{12}O_{40}$ acid.[19] Even though HPA is considered a super acid and is active in several organic reactions because of the high active Brønsted sites, the synthesized $Cs_{2.5}H_{0.5}PW_{12}O_{40}$/C was inactive

19390190, 0, Downloaded from https://onlinelibrary.wiley.com/doi/10.1002/cjce.25136 by Ecole Polytechnique De Montreal, Wiley Online Library on [24/11/2023]. See the Terms and Conditions (https://onlinelibrary.wiley.com/terms-and-conditions) on Wiley Online Library for rules of use; OA articles are governed by the applicable Creative Commons License

for this chemistry (TBA conversion and TBHP selectivity of 8% and 9%, respectively—Figure 5). We attribute this to the alkaline nature of the catalytic support and the uneven distribution of the HPA over the support surface due to high HPA concentrations (Figure 6).[44]

Powder activated carbon is more active than granule particles as the high surface availability is capable of adsorbing more H_2O_2 than creating HOO.[37,45] However, the non-dissociated H_2O_2 reacts again with the HOO. radical and degrades to water and oxygen[46]:

$$AC + H_2O_2 \rightarrow AC^+ + OH^- + OH^{\cdot} \quad (11)$$

$$AC^+ + H_2O_2 \rightarrow AC + HOO^{\cdot} + H^+ \quad (12)$$

$$H_2O_2 + HOO^{\cdot} \rightarrow OH^{\cdot} + H_2O + O_2 \quad (13)$$

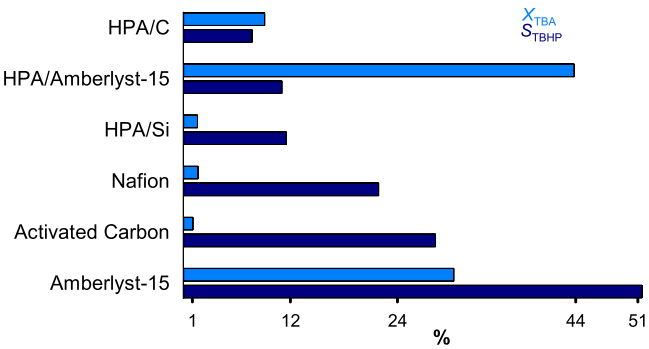

FIGURE 5 Distribution of the *tert*-butyl alcohol (TBA) conversion, *tert*-butyl hydroperoxide (TBHP) selectivity, and yield for the different tested catalysts at 1 h. HPA, heteropoly acids.

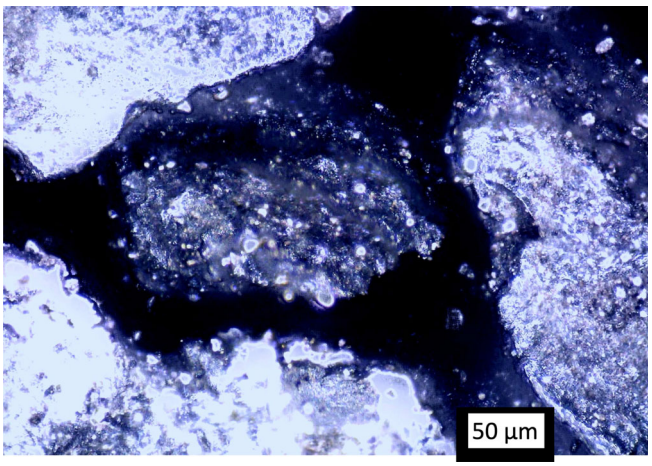

FIGURE 6 Microscope picture of the $Cs_{2.5}H_{0.5}PW_{12}O_{40}$/C catalyst. The glossy points represent the heteropoly acid salt while the black particles are the carbon support.

However, because of the limitations in the fixed bed reactor, our design was constrained to the larger granules. The low selectivity/activity was due in a part to the larger particles but also to the degradation of H_2O_2 to H_2O and O_2 (Equation 13). TBA does adsorb to the activated carbon but the concentration of the HOO. radicals is insufficient to form TBHP.

Finally, the combination of both HPA and Amberlyst-15 was predicted to have higher activity than Amberlyst-15 due to the double interaction and strength of Brønsted acidic sites. Unfortunately, this was not the case and the $Cs_{2.5}H_{0.5}PW_{12}O_{40}$/Amberlyst-15 yielded 6% of TBHP (Figure 5). This is because we did not wash away the sulfonated groups before impregnation of HPA. That way, the HPA and sulfonic groups are both present on the support and compete on the TBA adsorption, instead of just having the stronger HPA.

3.6 | Kinetics

We can express the reaction of TBHP as the function of the concentrations of TBA and H_2O_2 raised to the power α and β respectively:

$$\frac{d[\text{TBHP}]}{dt} = -\frac{d[\text{TBA}]}{dt} = k' \cdot [\text{TBA}]^{\alpha} \cdot [H_2O_2]^{\beta} \quad (14)$$

where k' is the kinetic rate constant. Since H_2O_2 is in excess (and constant), we combine it with k to give: $k = k' \cdot [H_2O_2]^{\beta}$ and a new equation:

$$\frac{d[\text{TBHP}]}{dt} = -\frac{d[\text{TBA}]}{dt} = k \cdot [\text{TBA}]^{\alpha} \quad (15)$$

We assumed a first order rate expression ($\alpha = 1$) and found that the model agrees with the experimental data between 30 and 50°C (Figure 7). The turn over frequency (TOF) was approximately 0.03 min^{-1}, which is consistent with acidic catalysts that vary from 0.001 to 0.7 min^{-1}.[47] At 60 and 70°C, the experimental data deviate especially at longer time (Figure 8). Presumably, other by-products form but are not detected with the GC. DTBP undergoes thermal and acid-catalyzed decomposition at higher temperature to stable radicals and molecules like methane, ethane, water, 2-methyl propane, ethane, and so forth.[24,48]

We derived the activation energy from the model (Equation 16) between 30 and 50°C and obtained a value of 32 kJ mol^{-1}.

$$k = 0.003 \exp\left[-\frac{32{,}000}{R}\left(\frac{1}{T} - \frac{1}{323}\right)\right] \quad (16)$$

1939019x, 0, Downloaded from https://onlinelibrary.wiley.com/doi/10.1002/cjce.25136 by Ecole Polytechnique De Montreal, Wiley Online Library on [24/11/2023]. See the Terms and Conditions (https://onlinelibrary.wiley.com/terms-and-conditions) on Wiley Online Library for rules of use; OA articles are governed by the applicable Creative Commons License

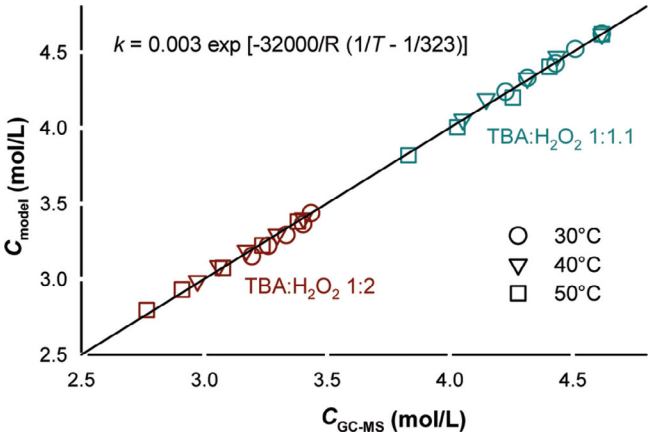

FIGURE 7 Parity plot showing the extent of model's accuracy (*tert*-butyl alcohol [TBA] concentrations of 4.62 and 3.44 mol L^{-1}.

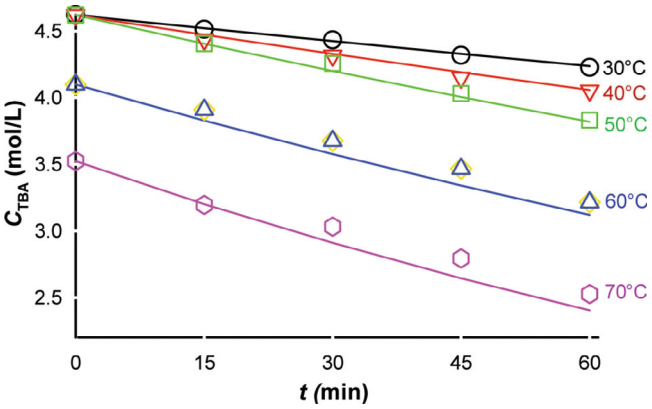

FIGURE 8 Plot of $\ln(C_{TBA})$ versus time at T between 30 and 70°C and molar ration of 1.1. The line represents the model. TBA, *tert*-butyl alcohol.

When applying the steady state approximation on $H_3C-\overset{CH_3}{\underset{CH_3}{C^{\cdot}}}$ radical and knowing that the formation of this radical is the rate determining step, the rate of the reaction is $r = k_1 \cdot [\text{TBA}]$. This expression conforms with the obtained kinetic results that show the pseudo-first order in TBA. If the first reaction is slow, that means the contribution of $H_3C-\overset{CH_3}{\underset{CH_3}{C^{\cdot}}}$ and HO^- toward TBA can be neglected in front of TBHP synthesis. Additionally, the *tert*-butoxy radical is more likely to react with HOO^- and produce TBHP than with HO^- to give back TBA.

4 | CONCLUSIONS

Amberlyst-15 catalyst, H_2O_2 partially oxidizes TBA to products to be TBHP, DTBP, and peroxyketal. Yields were much higher with Amberlyst-15 than the other five catalyst compositions tested. Its Brønsted acid sites account for the high activity. However, yield is lower than for the homogeneous process with H_2SO_4 as a catalyst that exceeds 90%[49] in laboratory vessels or the partial oxidation of isobutane that approaches 30%.[50] We showed that the Eley–Rideal model that is first order in TBA with an activation energy of 32 kJ mol^{-1} explains the variance in the data adequately from 3050°C. However, further experiments at lower and higher H_2O_2 concentrations are required to substantiate the model. We anticipate improved yield with a larger fixed-bed reactor in recycle mode and higher inventories of Amberlyst-15 to increase the number of acidic sites. Increasing temperature to improve yield favours parasitic reactions, particularly if the stainless steel walls are not passified or coated with an inert. At 70°C, the yield of DTBP increased from 0.4% to >6% at a flow rate of 1 mL min^{-1} versus <2 mL min^{-1}. The yield was essentially invariant with temperature at all other conditions, indicating that any reaction due to the steel reactor was negligible.

AUTHOR CONTRIBUTIONS

Marie-Thérèse El Kfoury: Conceptualization; investigation; methodology; visualization; formal analysis; data curation; writing – original draft. **Olga V. Chub:** Conceptualization; investigation; writing – original draft; methodology; formal analysis; supervision. **Daria C. Boffito:** Data curation; formal analysis; writing – review and editing; validation. **Gregory S. Patience:** Conceptualization; investigation; funding acquisition; writing – original draft; writing – review and editing; visualization; validation; formal analysis; project administration; resources; supervision; methodology.

ACKNOWLEDGEMENTS

We acknowledge Arkema U.S. for their funding and support.

PEER REVIEW

The peer review history for this article is available at https://www.webofscience.com/api/gateway/wos/peer-review/10.1002/cjce.25136.

DATA AVAILABILITY STATEMENT

The data that support the findings of this study are available from the corresponding author upon reasonable request.

1939019x, 0, Downloaded from https://onlinelibrary.wiley.com/doi/10.1002/cjce.25136 by Ecole Polytechnique De Montreal, Wiley Online Library on [24/11/2023]. See the Terms and Conditions (https://onlinelibrary.wiley.com/terms-and-conditions) on Wiley Online Library for rules of use; OA articles are governed by the applicable Creative Commons License

ORCID

Gregory S. Patience https://orcid.org/0000-0001-6593-7986

REFERENCES

[1] A. Uhl, M. Bitzer, H. Wolf, D. Hermann, S. Gutewort, M. Völkl, I. Nagl, *ULLMANN'S Encyclopedia of Industrial Chemistry*, Wiley-VCH Verlag GmbH, Weinheim, Germany **2017**, p. 1.
[2] K. Pulidindi, A. Prakash, Organic peroxide market size, share and industry analysis report by product (ketone peroxide, diacyl peroxides, dialkyl peroxide, percarbonates, hydro peroxides, peroxyesters) and application (polymer, coatings and adhesives, paper and textiles, cosmetics, rubber, healthcare), regional outlook, growth potential, competitive market share and forecast, 2021–2027. **2021** Https://www.gminsights.com/industry-analysis/organic-peroxide-market (accessed: July 2022).
[3] J. Sanchez, T. N. Myers, *Kirk-Othmer Encyclopedia of Chemical Technology*, Wiley, Hoboken, MA **2000**, p. 1.
[4] S. K. Kyasa, *PhD Thesis*, University of Nebraska (Nebraska, Lincoln) **2015**.
[5] M. A. Mueller, J. R. Sanderson, *U.S. Patent 5,395,980*. **1995**.
[6] W. E. Vaughan, F. F. Rust, *U.S. Patent 2,403,772*. **1946**.
[7] E. R. Bell, W. E. Vaughan, *U.S. Patent 2,630,456*. **1949**.
[8] N. A. Milas, *U.S. Patent 2,223,807*. **1940**.
[9] P. Frenkel, T. Pettijohn, *Eeuropean patent 1,305,283/b1*. **2006**.
[10] G. Gelbard, *Ind. Eng. Chem. Res.* **2005**, *44*, 8468.
[11] G. A. G. A. Olah, G. S. Prakash, A. Molnar, J. Sommer, *Superacid Chemistry*, 2nd ed., Wiley, Hoboken, MA **2009**.
[12] R. Pal, T. Sarkar, S. Khasnobis, *ARKIVOC* **2012**, *13*, 570.
[13] K. Kreuer, M. Ise, A. Fuchs, J. Maier, *J. Phys. IV* **2000**, *10*, 7.
[14] A. Kusoglu, A. Z. Weber, *Chem. Rev.* **2017**, *117*, 987.
[15] M. A. Modestino, D. K. Paul, S. Dishari, S. A. Petrina, F. I. Allen, M. A. Hickner, K. Karan, R. A. Segalman, A. Z. Weber, *Macromolecules* **2013**, *46*, 867.
[16] P. P. Sharma, D. Kim, *Membranes* **2022**, *12*, 521.
[17] H. Firouzabadi, A. A. Jafari, *J. Iran. Chem. Soc.* **2005**, *2*, 85.
[18] M. M. Heravi, M. V. Fard, Z. Faghihi, *Green Chem. Lett. Rev.* **2013**, *6*, 282.
[19] V. Calvino-Casilda, A. J. Lopez-Peinado, C. J. Duran-Valle, R. M. Martin-Aranda, *Catal. Rev.: Sci. Eng.* **2010**, *52*, 325.
[20] Y.-W. Wang, C.-M. Shu, *Ind. Eng. Chem. Res.* **2010**, *49*, 8959.
[21] Y.-W. Wang, *Ind. Eng. Chem. Res.* **2012**, *51*, 7845.
[22] R. Andreozzi, V. Caprio, S. Crescitelli, G. Russo, *J. Hazard. Mater.* **1988**, *17*, 305.
[23] T. Willms, H. Kryk, J. Oertel, C. Hempel, F. Knitt, U. Hampel, *Thermochim. Acta* **2019**, *672*, 25.
[24] N. Sebbar, J. W. Bozzelli, H. Bockhorn, *Int. J. Chem. Kinet.* **2015**, *47*, 133.
[25] T. Willms, H. Kryk, J. Oertel, X. Lu, U. Hampel, *J. Therm. Anal. Calorim.* **2017**, *128*, 319.
[26] E. J. Mistrik, J. Kostal, *Chem.-Tech. (Heidelberg, Ger.)* **1977**, *29*, 388.
[27] S. Soled, S. Miseo, G. Mcvicker, W. E. Gates, A. Gutierrez, J. Paes, *Catal. Today* **1997**, *36*, 441.
[28] S. J. Yang, X. X. Du, L. He, J. T. Sun, *Journal of Zhejiang University: Science* **2005**, *6*, 373.
[29] T. Baba, Y. Ono, *Appl. Catal.* **1986**, *22*, 321.
[30] A. Purwaningsih, A. N. Kristanti, D. Z. Mardho, D. W. Saraswati, N. M. Putri, N. H. Saputri, H. Hartati, *IOP Conference Series: Earth and Environmental Science* **2019**, *217*, 012002.
[31] Z. Rappoport Ed., *The Chemistry of Peroxides*, John Wiley and Sons, Ltd, Hoboken, MA **2006**.
[32] H. Laajimi, F. Galli, G. S. Patience, D. Schieppati, *Can. J. Chem. Eng.* **2022**, *100*, 3123.
[33] *Tert-butanol*. **2022** https://pubchem.ncbi.nlm.nih.gov/compound/tert-Butanol (accessed: June 2023).
[34] *Tert-butyl hydroperoxide*. **2022** https://pubchem.ncbi.nlm.nih.gov/compound/Tert-butyl-hydroperoxide (accessed: June 2023).
[35] *Di-tert-butyl peroxide*. **2022** https://pubchem.ncbi.nlm.nih.gov/compound/Di-tert-butyl-peroxide (accessed: June 2023).
[36] Systat, SigmaPlot 12.5 User's Guide Part 3, Systat Software, San Jose, CA **2013**.
[37] Q. Zhao, Q. Mao, Y. Zhou, J. Wei, X. Liu, J. Yang, L. Luo, J. Zhang, H. Chen, H. Chen, L. Tang, *Chemosphere* **2017**, *189*, 224.
[38] H. C. Dong, T. H. Ho, T. M. Nguyen, Y. Kawazoe, H. M. Le, *J. Comput. Chem.* **2021**, *42*, 1344.
[39] H. B. El-Nassan, *Russ. J. Org. Chem.* **2021**, *57*, 1109.
[40] Lyondell Chemical Company, *T-hydro tert-butyl hydroperoxide (tbhp) product safety bulletin*. www.lyb.com (accessed: June 2022).
[41] D. Cavuoto, F. Zaccheria, N. Ravasio, *Catalysts* **2020**, *10*, 1337.
[42] R. Tesser, M. D. Serio, L. Casale, G. Carotenuto, E. Santacesaria, *Can. J. Chem. Eng.* **2010**, *88*, 1044.
[43] M. M. Talukder, J. C. Wu, S. K. Lau, L. C. Cui, G. Shimin, A. Lim, *Energy Fuels* **2009**, *23*, 1.
[44] M. J. D. Mahboub, G. S. Patience, in *Industrial Green Chemistry* (Eds: J.-L. Dubois, S. Kaliaguine), de Gruyter, Berlin **2020**, p. 1.
[45] A. Georgi, F. D. Kopinke, *Appl. Catal., B* **2005**, *58*, 9.
[46] A. Flouret, M. C. de Almeida, T. F. de Oliveira, F. P. de Sá, *Can. J. Chem. Eng.* **1979**, *2018*, 96.
[47] I. E. Wachs, *J. Catal.* **2022**, *405*, 462.
[48] P. R. Dluzneski, *Rubber Chem. Technol.* **2001**, *74*, 451.
[49] X. Yue, J. J. Yao, L. Liao, X. Q. Yu, D. C. Liu, *Yingyong Huagong* **2008**, *37*, 808.
[50] A. J. Arpe, *Industrielle Organische Chemie Bedeutende Vor-Und Zwischenprodukte*, Wiley-VCH Verlag GmbH & Co., Berlin **2007**.

How to cite this article: M.-T. El Kfoury, O. V. Chub, D. C. Boffito, G. S. Patience, *Can. J. Chem. Eng.* **2023**, 1. https://doi.org/10.1002/cjce.25136

1939019x, 0, Downloaded from https://onlinelibrary.wiley.com/doi/10.1002/cjce.25136 by Ecole Polytechnique De Montreal, Wiley Online Library on [24/11/2023]. See the Terms and Conditions (https://onlinelibrary.wiley.com/terms-and-conditions) on Wiley Online Library for rules of use; OA articles are governed by the applicable Creative Commons License